Determination of breakage rates with single drop experiments

Sebastian Maaß[1*], *Stephanie Hermann*[1], *Matthias Kraume*[1]

[1]*Technische Universität Berlin, Straße des 17. Juni 135, Sekr. MA 5-7, Chair of Chemical and Process Engineering, Sekr. MA 5-7, 10623 Berlin, Germany*

[*]*corresponding author (sebastian.maass@tu-berlin.de)*

Abstract – In this study, detailed and precise parameter determination for the PBM models of the breakage rates have been analyzed separately from coalescence in a single drop breakage cell. Therefore the breakage time and the breakage probability of toluene and petroleum drops have been studied using high-speed imaging. Additionally the number of daughter fragments occurring in single drop breakage events has been observed. All results have been compared with values from literature. The single drop experiments support the assumption of binary breakage as of increasing breakage time with increasing mother drop diameter.

Keywords – drop breakage, population balance modeling, breakage kernel model, breakage time, number of daughter drops, parameter estimation, Rushton turbine

1 Introduction

The dispersion of an immiscible fluid in a turbulent liquid flow is commonly found in many technical as well as natural processes, with major importance for the chemical, pharmaceutical, mining, petroleum, and food industries. The size distribution of the drops resulting from the opposed phenomena of turbulent drop breakage and coalescence plays an essential role in the overall performance of these processes. Complete models for the drop size distribution as a function of power input, material and process parameters are rare and relatively inaccurate.

An extremely useful modeling approach is population balance modeling (PBM). It has been widely used to predict drop size distributions in several applications (Ramkrishna 2000). The key challenge associated with the formulation of predictive PBM models is experimental determination of unknown drop breakage and coalescence function. While drop breakage under laminar conditions has been extensively studied, predictive models for drop breakage and coalescence under turbulent conditions are lacking or rather imprecise (Raikar et al. 2009). Many contradictory ideas for breakage and coalescences rates have been published over the last decades. A broad and detailed overview of existing functions is given by Liao and Lucas (Liao and Lucas 2009; Liao and Lucas 2010).

In this work we want to focus on analyzing drop breakage and daughter drops in turbulent flows. The number of daughter drops ν has got little attention over the last decades and is generally assumed as two for the binary breakage (Hill and Ng 1995;

Raikar et al. 2009) to avoid complications associated with modeling multiple daughter drop formations. This, in its absolute meaning, is in contradiction with experimental results in stirred tanks (Hancil and Rod 1988; Kuriyama et al. 1995) and on single drops (Maaß et al. 2007). The modeling of the breakage rate $g(d_p)$ has received considerable attention and a broad variety of functional forms are available (see Liao and Lucas (2009) and also Lasheras et al. (2002) for a detailed overview).

The breakage of drops in turbulent dispersions is determined by the continuous phase hydrodynamics and interfacial interactions. While many particle breakup mechanisms are discussed and described in literature, we consider the breakup of fluid particles as mainly being caused by turbulent pressure fluctuations along the surface, or by drop-eddy collision (Liao and Lucas 2009). Therefore, we will only focus on approaches based on those mechanisms. Nevertheless, breakage rates provided by various authors, based on the same major assumptions, are still inconsistent. More recent models give a monotonic relation between the breakup frequency and the drop size while the older ones exhibit a maximum as the parent diameter increases, which is already considered erroneous in literature (Chen et al. 1998; Tsouris and Tavlarides 1994). However, the argument is open to question. Additionally the quantitative difference between PBM models can achieve several orders of magnitudes and needs to be fixed through parameter adaptation. For more detailed understanding and precise parameter determination, breakage rates will be analyzed in this study separately from coalescence in a single drop breakage cell (Maaß et al. 2007).

2 Drop breakage in turbulent systems

Numerous experiments and simulations of single fluid particle deformation and breakage have been carried out in parallel bands or cylinder devices. The experiments as the simulations were carried out at low (Windhab et al. 2005) and high Reynolds numbers. The advantages of detailed drop break-up experiments under steady and transient shear or elongation, as well as mixed flow conditions at low Reynolds numbers, are obvious. The extremely well defined conditions allow a clear connection of the flow field and the particle deformation as well as breakage mechanisms. Additionally, the numerical results can precisely be evaluated. At these conditions with the combination of experiments and simulations of the flow field, the particle tracking procedure along distinct particle flow tracks allows the quantification of the transient drop deformation history of selected drops along their paths through such apparatus. These insights allow improved design, scale-up or optimization of dispersing apparatus, for example of high viscous fluids, but lack applicability to low viscous systems with high turbulence.

Although desirable, numerical simulations of anisotropic turbulent drop breakage are extremely expensive in computing time due to the wide range of length scales and unsteadiness that characterizes turbulence. A first simplification is the analysis of such events in jet streams through a nozzle (Eastwood et al. 2004). The mean velocities and the turbulence properties are here symmetrically distributed, which simplifies the modeling. Rodríguez-Rodríguez et al. (2006) studied numerically the breakup process of a drop immersed in such a straining flow at high Reynolds numbers. Despite the simplicity of the model, it qualitatively displays some of the features of the turbulent breakup of drops. However, the aim of this investigation is the validation of breakage models used for simulations of drop sizes in stirred vessels

with anisotropic turbulence and determination of the according numerical constants used in those models.

2.1 Modeling of drop breakage

The mechanistic model for the rate of drop breakage proposed by Coulaloglou and Tavlarides (1977) is based on the assumption that $g(d_P)$ is a product of the fraction of the total number of breaking drops, and the reciprocal time needed for the drop breakage to occur:

$$g(d_P) = \left(\frac{1}{\text{breakage time}}\right) \cdot \left(\frac{\text{fraction of}}{\text{breaking drops}}\right) = \frac{1}{t_{break}} \cdot \frac{N_{break}}{N_{tot}} \qquad (1)$$

The fraction of drops breaking can be measured directly in the breakage channel and is assumed to be proportional to the fraction of turbulent eddies colliding with the drops that have a turbulent kinetic energy greater than the drop surface energy. The drop breakage time is estimated by assuming that it is approximately equal to the characteristic time for drop deformation and derived from Batchelor's equation for the motion of two lumps in the turbulent field. The increasing distance between the two lumps or particles is proportional to the time, the energy dissipation rate ε and the initial distance of the measurement, which is equal to t_{break} for a drop breakage event.

$$\left(\overline{AB'}(t)\right)^2 \propto \left(\overline{AB} \cdot \varepsilon\right)^{2/3} \cdot t \text{ , with } \overline{AB}(t = t_{break}) \qquad (2)$$

For equal size daughter drops after a binary breakage, the distance between both daughter particles is equal to their diameter d'_P, which is equal to d''_P. With this assumption and an introduced proportionality constant c, the breakage time can be calculated with the following equation:

$$t_{break} = c \cdot \frac{d_P^{2/3}}{\varepsilon^{1/3}} \qquad (3)$$

Including the turbulence damping dispersed phase fraction φ, the overall breakage rate is written as following:

$$g(d_p) = c_{1,break} \frac{\varepsilon^{1/3}}{(1+\varphi_d) d_P^{2/3}} \exp\left(-c_{2,break} \frac{\gamma(1+\varphi_d)^2}{\rho_d \, \varepsilon^{2/3} d_P^{5/3}}\right), \; c_{1,break}, c_{2,break} \, [-]. \qquad (4)$$

Although Coulaloglou and Tavlarides (1977) reported a dependence of breakage probability (exponential term in equation (4)) on the disperse phase density, ρ_d, Lasheras et al. (2002) criticizing this in general and postulating that the dependence should be on the continuous phase density, ρ_c. Vankova et al. (2007) are taking this thesis into account and are extending equation (4) by the mass densities, opposed to the critics by Lasheras et al. (2002) in the pre-exponential term for dispersed phases with low viscosities:

$$g(d_p) = c_{1,break} \frac{\varepsilon^{1/3}}{(1+\varphi_d) d_P^{2/3}} \sqrt{\frac{\rho_d}{\rho_c}} \exp\left(-c_{2,break} \frac{\gamma(1+\varphi_d)^2}{\rho_d \, \varepsilon^{2/3} d_P^{5/3}}\right), \; c_{1,break}, c_{2,break} \, [-], \qquad (5)$$

this is still very similar to the original equation proposed by Coulaloglou and Tavlarides (1977). Also Raikar et al. (2009) extended the model in equation (4). They

introduced the dispersed mass density in the pre-exponential term, describing the breakage time as follows:

$$t_{break} = c \cdot \frac{d^{2/3}}{\varepsilon^{1/3}} \cdot \rho_d^{1/3},\ c\ [kg^{1/3} \cdot m^{-1}] \qquad (6)$$

The dimension of the numerical constant c has to be adapted by this extension to $kg^{1/3} \cdot m^{-1}$. In contradiction to these works is the assumption of Chen et al. 1998, whose set the breakage time as a constant but introduced the dispersed phase viscosity into the formulation of the breakage probability P, to take into account drop viscoelasticity:

$$P = \frac{N_{break}}{N_{tot}} = \exp\left(- \frac{c_{2,break}\,\gamma (1+\varphi)^2}{\rho_d d_P^{5/3} \varepsilon^{2/3}} - \frac{c_{3,break}\,\eta_d (1+\varphi)}{\rho_d d_P^{4/3} \varepsilon^{1/3}} \right),\ c_{2,break},\ c_{3,break}\ [-]. \qquad (7)$$

Equation (7) is a monotone growing function and contains the influence of viscosity in contrast to the model of Coulaloglou and Tavlarides (1977). However, the presented equations (4)-(7) are mechanistic models.

Another class of models considers the random splitting of the initial mother drop in various disjointed elements in one or several steps. A key assumption, introduced by Narsimhan et al. (1979), is that the breaking drops form a Poisson process. That was generally criticized by Villermaux (2007). He stated that nature does not split liquid volumes at random. With experimental high-speed images of breaking drops he showed that minute but significant differences exist between experimental data and assumed stochastic distributions, like Poisson or log-normal distributions (Villermaux 2007).

However, the breakage rate of Narsimhan et al. (1979) was used by several authors for good drop size prediction results and its stochastic nature was already overworked in two steps by Alopaeus et al. (2002). Firstly they combined the original kernel with the consideration of viscous forces (see second term under the square root in equation (8)) according to Calabrese et al.(1986), while the original development was based on the assumption that viscous forces are negligible.

$$g(d_p) = c_{1,break}\,\varepsilon^{1/3} \cdot \mathrm{erfc}\left(\sqrt{ \frac{c_{2,break}\,\gamma}{\rho_c d_P^{5/3} \varepsilon^{2/3}} + \frac{c_{3,break}\,\eta_d}{\sqrt{\rho_c \rho_d}\, d_P^{4/3} \varepsilon^{1/3}} } \right)\ c_{1,break}\ [m^{-2/3}];\ c_{2,break},\ c_{3,break}\ [-]. \qquad (8)$$

Secondly they enhanced the pre erfc-term. The equation was modified including the ε dissipation dependence for the eddy-drop collision part. They found a dependency of $\varepsilon^{1/3}$ in the pre erfc-parameter, which is also predicted by turbulence theory. No significant diameter dependency for $c_{1,break}$ in equation (8) was found (Alopaeus et al. 2002). Note that by this extension the original dimension of the numerical constant $c_{1,break}$ has to be changed from $[s^{-1}]$ to $[m^{-2/3}]$.

Although Alopaeus et al. (2002) are not specifically determining a physical meaning of the pre-erfc-term and the erfc-term, a closer examination and a comparison with the drop breakage probability from Chen et al. (1998) in equation (7), reveals an interesting similarity. The physical description of the drop breakage event controlled by the surface and viscous forces described by both author groups are absolute equal. Additionally the pre-erfc-term with the dimension s^{-1} and the dependency on ε

(see equation (8)) reveals many similarities with the original introduced breakage time by Coulaloglou and Tavlarides (1977). Therefore the model of Alopaeus et al. (2002) can also be included into a divided comparison of different model approaches for breakage probability and the breakage time.

Martínez-Bazán et al.(1999) proposed a breakage model for bubbles based on kinematic ideas (energy balance).The basic thesis is that for a droplet to be split, the turbulent stresses should over come the deformation energy to modify the surface. If viscous forces are neglected, the confinement stress is defined as:

$$g(d_p) = \frac{1}{t_{break}} = c_{1,break} \frac{\sqrt{c_{2,break} (\varepsilon \cdot d_P)^{2/3} - (12\gamma)/(\rho_c d_P)}}{d_P}, \; c_{1,break}, c_{2,break} [-] \qquad (9)$$

Here $c_{2,break}$ is 8.2 given by Batchelor (1956) and based on homogenous turbulence, which was fulfilled in the experimental work of Martínez-Bazán et al. (1999). The parameter $c_{1,break}$ in equation (9) has been found experimentally as 0.25. The breakage rate is zero for particles of size $d_P \leq d_{P,crit}$, and it increases rapidly for drops larger than the critical one, $d_P \geq d_{P,crit}$ (Martínez-Bazán et al. 1999).

The model has many similarities to the previous five models. The significant difference is the discarding of probability theory for the distribution of kinetic energy or velocity fluctuation. Conversely to the model of Alopaeus et al. (2002) and Chen et al. (1998) with a monotonic increase of the drop breakage with increasing diameter, the model predicts a maximum a certain drop diameter. This maximum is reached at $d_{P,max} = 1.63 d_{P,crit}$. The maximum of $g(d_P)$ according to Martínez-Bazán (1999) is a function of the energy dissipation rate and the interfacial tension:

$$g_{max}(d_p) = f(\varepsilon, \gamma) \propto \left(\frac{\gamma}{\rho}\right)^{-2/5} \varepsilon^{3/5} \qquad (10)$$

Although the model describes not only the corresponding single bubble experiments qualitatively but also quantitatively with remarkable deviation always lower then 10 percent, it is restricted to homogenous and isotropic turbulent flows and contains still two adjustable parameters. Especially the parameter $c_{2,break}$ in equation (9), derived from Batchelor (1956) and mentioned as a theoretical constant, will be different for stirred vessels due to the inhomogeneous flow field.

The dispersed phase fraction, a process parameter with major importance for industrial applications, is taken into account in some of the models. Its effect is always modeled as a turbulence damper. Due to the low influence of single drops on the flow field and the turbulence due to the extreme low corresponding dispersed phase fraction, those terms will be negligible for further model analysis.

2.2 Experimental investigations

Ideally, all models already described require a detailed mapping of the energy dissipation rate throughout the system. Additionally the preciseness of the models is, if the energy dissipation is well characterized, directly related to the preciseness of the modeling of the particle-eddy interaction. To avoid those uncertainties experimental based breakage kernels have been published. They are either obtained by direct observing of breakage events (Konno et al. 1983) or by direct calculations

based on experimental results, using the inverse-problem approach (Sathyagal et al. 1995).

Konno et al. (1983) used high-speed photography to directly observer drop breakage events in stirred vessels. To avoid coalescence he always used a dilute liquid/liquid system with a dispersed phase fraction lower then 0.2 %. The images were taken with up to 4000 fps. The breakage time, drop path and the number of drops per breakage event were recorded. The investigated mother drops size are in the range of 0.26 - 1.0 mm. Breakage times always lower than 7 ms were observed by Konno et al. (1983). The major drawback of their approach is the insufficient number of breakage events for statistically meaningful results. For a strong varying mother drop diameter they measured less than a hundred breakage events. Bahmanyar and Slater observed breakage of single drops in a rotating disc contactor. The determined minimum energy dissipation rates under those, drops of a given size do not break. The mean number of daughter drops produced under breakage was correlated as a simple function of drop diameter based on the critical diameter and agreement were found with data from other types of agitated systems (Bahmanyar and Slater 1991). Based on the works of Hancil and Rod (1988) they correlate their number of daughter drops with equation (11):

$$\nu = 2 + 0.9\left[\left(d_P / d_{P,crit}\right) - 1\right] \qquad (11)$$

Starting at binary breakage the number of particles is increasing with increasing mother drop diameter d_P. Due to the low time resolution of their measurement techniques (capillary and video technique) they were not able to determine breakage times or the number of daughter drops connected to a single breakage event. Kuriyama et al. (1995) investigated single drop breakage events in stirred vessel, which were introduced via a loop flow into the stirrer zone. They analyzed the dependency of different high viscosities (0.1 – 12.6 Pa·s) on the number of daughter drops. Generally they observed a dependency of the number of daughter drops on the mother drop diameter. The direct proportionality was found over the whole viscosity range by using a viscosity correction term (see equation (12)).

$$\nu \propto \sqrt{\frac{\eta_d}{\eta_c}} \cdot {d_P}^{0.455} \qquad (12)$$

Andersson and Andersson (2006) investigated the dynamics of bubble and drop breakage with a high-speed technique. The breakage time, deformation and daughter drop size distribution were measured with frame rates of 1000 fps under homogenous turbulence. The highest values for the breakage time were found for the lowest flow velocity and the highest disperse viscosity of around $\bar{t}_{break}$ = 15 ms. The interpretation of the work by Anderson and Anderson (2006) is hard, while no definition for their breakage nor the overall amount of investigated events is given by the authors. However their rather qualitative then quantitative investigations propose binary breakage for bubbles but not for drops. The number of daughter drops for the dodecane/water system is decreasing with increasing energy dissipation. The absolute values for an average v of this system are given of around 3.2.

Table 1 – Results for the number of daughter drops for liquid/liquid systems

Literature reference	experimental set-up	used frame rate [fps]	number of daughter drops v [-]	dispersed viscosity η_d [mPa·s]
Konno et al. 1983	stirred vessel	4000	2.6 – 4.4	n/a
Chatzi and Lee 1987	stirred vessel	simulations	7	0.46
Kuriyama et al. 1995	loop reactor/ stirred vessel	n/a	4 – 27	100
Galinat et al. 2005	orifice flow	456	2 – 8	0.45
Andersson and Andersson 2006	static mixed reactor	1000	3.2	1.5

The works of Eastwood et al. (2004) are dealing with drop breakage in a turbulent liquid jet. They found that drops were considerably elongated before breakage. The deformation or stretching is increasing with increasing drop viscosity. The stretching occurred on scales comparable to the turbulent integral length scale, and some deformed drops seemed to rotate with the flow structures. They propose that the elongated particle break owing to capillary effects resulting from differences in the radius of curvature along their length. Therefore they scale the breakage time with the capillary time and draw similarities to laminar breakage. It was difficult for them to identify the number of fragments quantitatively but they stated that multiple break-up is most probable for their investigated system. Galinat et al. (2005) quantified this statement in a pipe flow for heptane drops by swarm and single drop experiments. They investigated the breakage probability, the number of daughter drops and the resulting daughter drop size distribution as a function of the flow velocity and mother drop diameter. The increase of both influence parameters lead to a strong increase of the breakage probability and the number of daughter drops. A summary for the different results in the different references on the number of daughter drops is given in Table 1.

Time resolved optical observations of breakage events need ultrahigh-speed imaging. The required frame rates are profoundly affected by the optical magnification of the imaging, which becomes clear when one considers that a velocity of 1 m/s correspond to 1 µm/µs (Thoroddsen et al. 2008). Therefore a summary for the number of daughter drops given in Table 1 always includes the used frame rate if mentioned in the according reference. Already this brief summary shows

that the assumption of binary breakage is a simplification which needs further attention.

3 Material and methods

3.1 Experimental set-up

For more detailed understanding and precise parameter determination, breakage rates have been analyzed separately from coalescence in a single drop breakage cell. In this set-up both the event of breakage and the daughter drop size distributions can be analyzed. A single blade representative for a section of a Rushton turbine is fixed in a rectangular channel. A single drop of a certain diameter between 500 and 3500 µm is introduced in a continuous flow. The relative velocity between blade and liquid flow was approximately 1.0 to 3.0 m/s, a range typical for the flow field around the stirrer in a stirred tank. Also the local energy dissipation rates of both, the channel and a stirred tank, were compared under the selected conditions. The dissipation rates and flow conditions in the stirred tank were in good agreement with those in the breakage channel (Maaß et al. 2009). Please also note the extensive description for the coordinate transformation of the rotating stirrer blade in a vessel into a fixed stirrer blade in the breakage channel in the named source.

Pictures of the single drop breakage event and the resulting daughter drops are taken with a high-speed camera using a frame rate of 822 frames per second (fps). Automated image recognition delivers results for the breakage time, number of daughter drops and daughter drop size distribution. Additionally the number of breaking drops is set into relation to the overall amount of investigated drops for one parameter set. This leads to experimentally determined breakage probabilities. The different steps of image processing and analysis are described in detail by Maaß et al. (2007). The former used software and the manual threshold setting is replaced by a full automation in MATLAB®, which uses analysis of the local grey value distribution to determine the right threshold for every sequence. Examples of the high-speed images are shown in Figure 3.

Table 2 – Listing of the data on used chemical media

	γ [mN/m]	γ [mN/m] with dye	ρ [kg/m³] at 20°C	η_d [mPa·s]	c_{dye} [g/L]
toluene	36	32	870	0.55	0.075
petroleum	42	38.5	790	0.65	0.075

The two organics used as dispersed phase for this investigation are toluene (99.98 % purity) and petroleum (99.9 % purity). Both were blended with a non-water soluble black dye, which decreases the interfacial tension between water and the organic but increases the optical evaluation possibilities. The influence on the interfacial tension was quantified using the pendant drop method (Jon et al. 1986). The chemical data for the used systems are listed in Table 2. It is important to mention, that petroleum is

a mixture and not a pure liquid. It has different names; while it is called petroleum in Germany, it is called kerosene in American English and paraffin oil in British English. Due to the origin of the researcher we will continue to use the term petroleum.

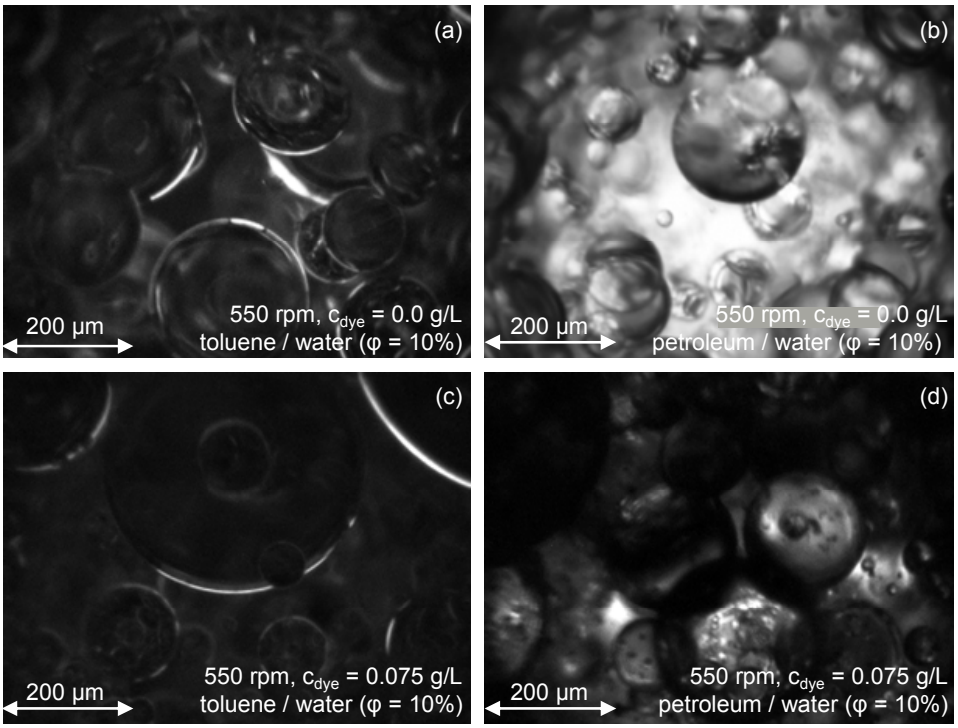

Figure 1 – Example photos of the analyzed chemical media in a stirred vessel, with and without dye.

Experiments in a standard stirred vessel (vessel diameter T = 150 mm, H/T = 1.0) were carried out to determine the influence of the used dye on the evolving drop sizes. The used photo-optical measurement technique and experimental set-up are explained in detail by Maaß et al. (2010) (see example images in Figure 1). The images are analyzed through a fully automated program, the used algorithm and working procedure is described in Maaß et al. (2011). Two example photos of the different drop swarms (always one with and one without dye) are shown for every used chemical media. The resulting cumulative number distributions after one minute of stirring are compared with each other in Figure 2. The presentation is in the probability density net that allows determining the shape of the distribution, which is Gaussian for all four cases. The distributions with dye are always wider than the ones without, for toluene and petroleum. Interestingly the influence of the dye causes additional small and large drops. This is probably related to the decrease in the interfacial tension and therefore increased breakage and coalescence rates parallel but at different diameter ranges. The breakage of small particles is increased as it is the coalescence of larger drops. The maximum deviation of the Sauter mean diameters ($d_{32} = \Sigma\ d_i^3/\Sigma d_i^2$) are less than 10% (see table in Figure 2). This is an appropriate deviation related to the enormous increase of possibilities in optical canalization.

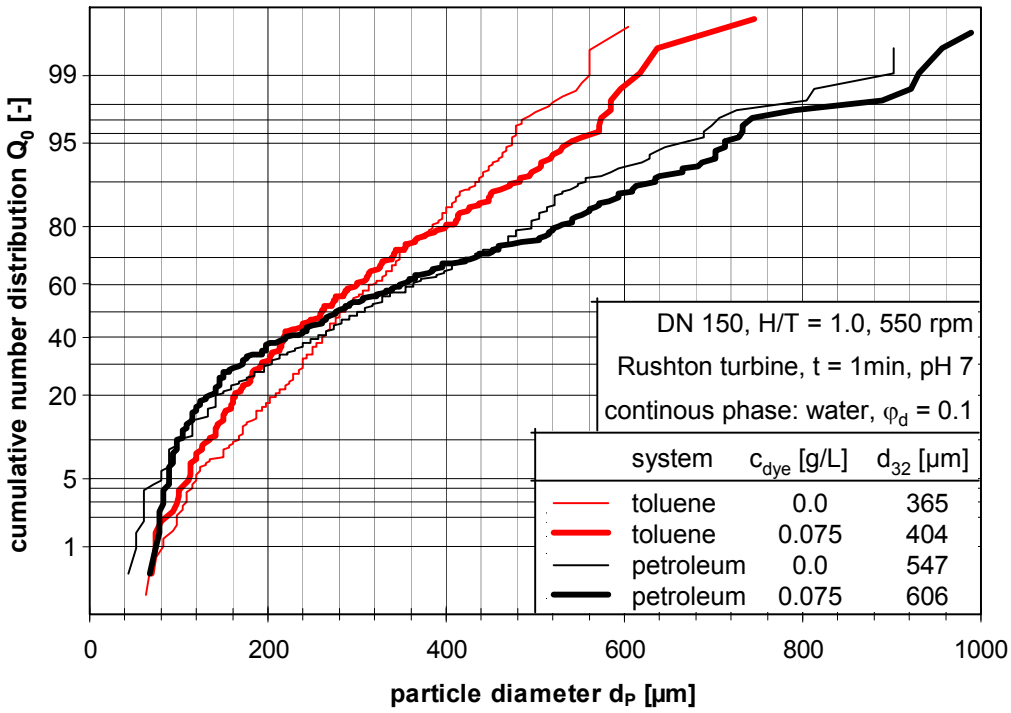

Figure 2 – Influence of the dye on the drop size distribution in a stirred vessel for both investigated dispersed phases, using a Rushton turbine.

Table 3 – Overview of the working program

system	flow velocity w [m/s]	mother drop diameter d_P [mm]
toluene/ water	1.0	1.0
	1.5	0.67, 1.0, 2.0, 3.0
	2.0	1.0
petroleum/ water	1.0	1.0
	1.5	0.54, 0.7, 1.0, 1.3, 1.9, 3.1
	2.0	1.0

The presented drop size distributions in Figure 2 also demonstrate the bandwidth of expected daughter drops. Therefore the mother drop sizes have been set between 500 and 3500 µm. The high accurate dosing pump produces mother drops with standard deviation of the diameter less than 0.003 mm (Maaß et al. 2009). An overview of the whole work program is given in Table 3. The influence of the flow

velocity and therewith the energy dissipation rate was varied for a constant mother drop diameter of 1.0 mm and the influence of the mother drop diameter was investigated for a constant flow velocity of 1.5 m/s. The influence of the viscosity and the interfacial tension was shown by parallel investigations with the two used dispersed phases.

3.2 Measurement procedure

For statistically firm conclusions, more than 1000 events are recorded for one parameter combination (constant drop diameter and flow velocity). Those experimental results generate the base for experimental determined breakage rates after the pioneer equation from Coulaloglou and Tavlarides (1977) (see equation (1)).The breakage probability is the relation between the number of all breaking drops and the complete parent population. Three sequences of example toluene drops (d_P = 1.0 mm, w = 1.5 m/s) are shown in Figure 3. The paths of three drops through the breakage channel are presented. Although the boundary conditions are the same, drop C is breaking but not the other two. Drop A and B going through the high turbulent region behind the stirrer blade, they are deformed by the colliding eddies – drop B even into a "peanut", but the surface forces are always stronger then the inertial forces. So the drops always stabilize and remain without break-up, an additionally control via a mass balance gives security for this results. That this behavior is not connected to the entrance coordinate is shown by the comparison of A and B. The not breaking drops are distributed over the channel entrance coordinate as the complete parent population (details for entrance distribution by Maaß et al. (2009)).

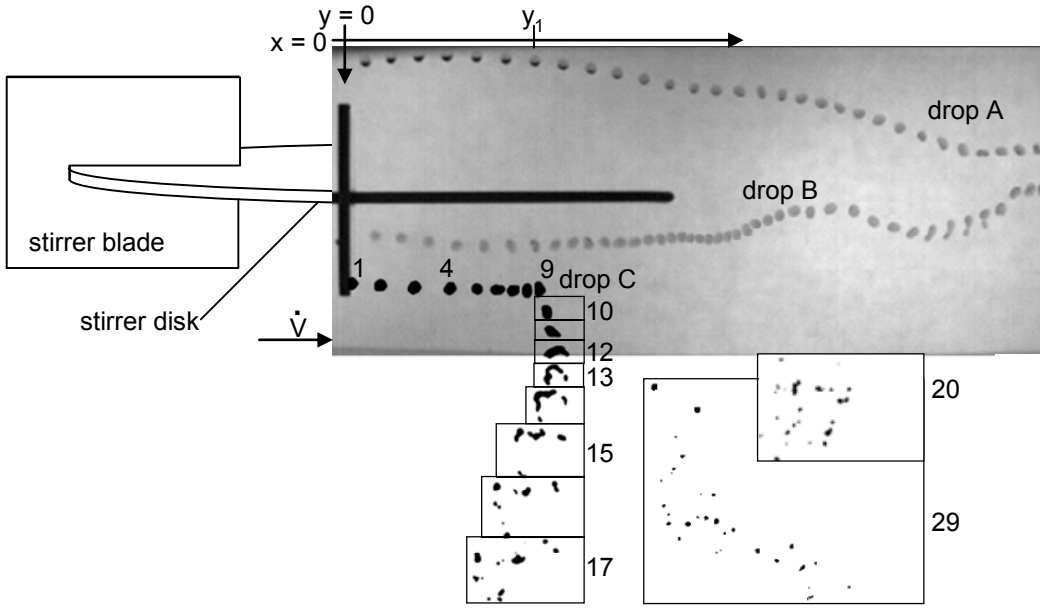

Figure 3 – Three example toluene drops (drop A and B – original images, drop C – after image processing), d_P = 1mm, w = 1.5 m/s, for the definition of the breakage time and for the breakage probability

Drop C represents a breaking drop after the image processing. The position of the particle can only be used until y_1. At this point and therefore after this time, the drop is caught in a local eddy. All eight framed following images remain at the same position and are only moved to represent a whole breakage event in Figure 3. The local eddies are deforming the particles. Thereby the drops are elongated until they go under a critical width to break. This moment (represented in Figure 3 with drop 13) is the time of the first breakage. Here the breakage time t_{break} is taken. The stirrer blade (y = 0, drop 1) marks the starting point for the timing of the first breakage. This delta in the images can be directly related to a time of the frame rate. With a frame rate of 822 fps the breakage time for example drop C can be calculated with equation (13).

$$t_{break} = \frac{\Delta \text{number of images}}{822\ \text{fps}} \qquad (13)$$

The breakage time for drop C is 0.016 seconds. Further more the number of daughter drops is determined. Two data are collected. The number of daughter drops right after the first breakage event (see 13 of drop C in Figure 3) and the maximum number of daughter drops occurring on one image during the complete breakage process (see 29 of drop C in Figure 3) are collected. They are later used to evaluate the assumption of binary breakage and the number of breakage events occurring in a row to one introduced mother particle.

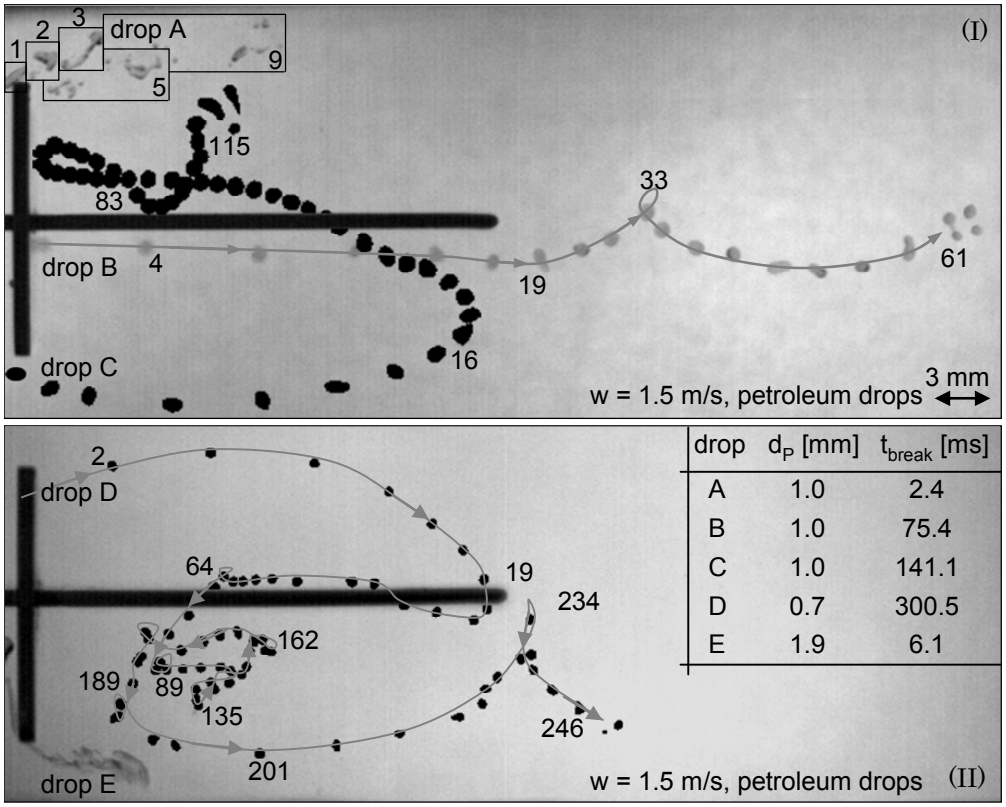

Figure 4 – Example high-speed images (original – drop A,B,E and after image processing – drop C,D) to illustrate the deviation of breakage time for constant stirrer speed and varying mother drop diameter

Figure 4 illustrates the influence of the inhomogeneous flow field on the breakage time. Part (I) of Figure 4 shows the path and therewith the breakage time of three equal sized mother drops at a constant flow velocity of 1.5 m/s. While example drop A is breaking on the second image due to the collision with the stirrer blade, Drop B is breaking after 75.4 ms, which is almost double the length of the average residence time for the presented flow velocity. Even more extreme is the path and breakage time of drop C. The drop is caught in a large eddy behind the blade, transported back, against the flow direction for more than 50 ms, caught again in a smaller eddy and then finally breaking after 141.1 ms, which is equal to 116 images. Part (II) illustrates the influence of the diameter on the breakage time. While drops are only broken by eddies equal and smaller their size (Shinnar 1961), the 0.7 mm drop (drop D) is breaking after a residence time of more than 300 ms. Opposed the 1.9 mm drop which is breaking directly at the stirrer blade. Those qualitative results are now quantified with the single drop experiment sets.

4 Results and Discussion

The experimental set-up has been qualified regarding the sensitivity to the temperature. All measurement were carried out at room temperature and an additional heating of the continous phase up to 40°C showed no significant influence on the breakage probability nor on the breakage time. In the following two chapters those terms will be analyzed in detail and compared with model approaches from literature. After determining optimal parameter for the presented model, all data will set together to calculate the breakage rate. Additionally the experimentally determined number of daughter fragments will be discussed at the end of this study.

4.1 Breakage probability

For a given set of system parameters, the breakage probability is defined as the ratio between the number of broken drops and the total number of injected drops of a given size (see equation (1)). The significance of the analyzed data set is always tested by cumulative averaging of the observed results over the number of investigated breakage events. Those results are given in Figure 5, for all investigated drop diameters. Petroleum and toluene drops are both presented there at a constant flow velocity of 1.5 m/s. As a general trend, the breakage probability increases with increasing mother drop diameter, for both analyzed systems. Note that due to the low breakage probabilities of the smallest investigated diameter, the overall number of investigated breakage event was increased to gain enough breaking drops. This was necessary for statistical significant breakage time results.

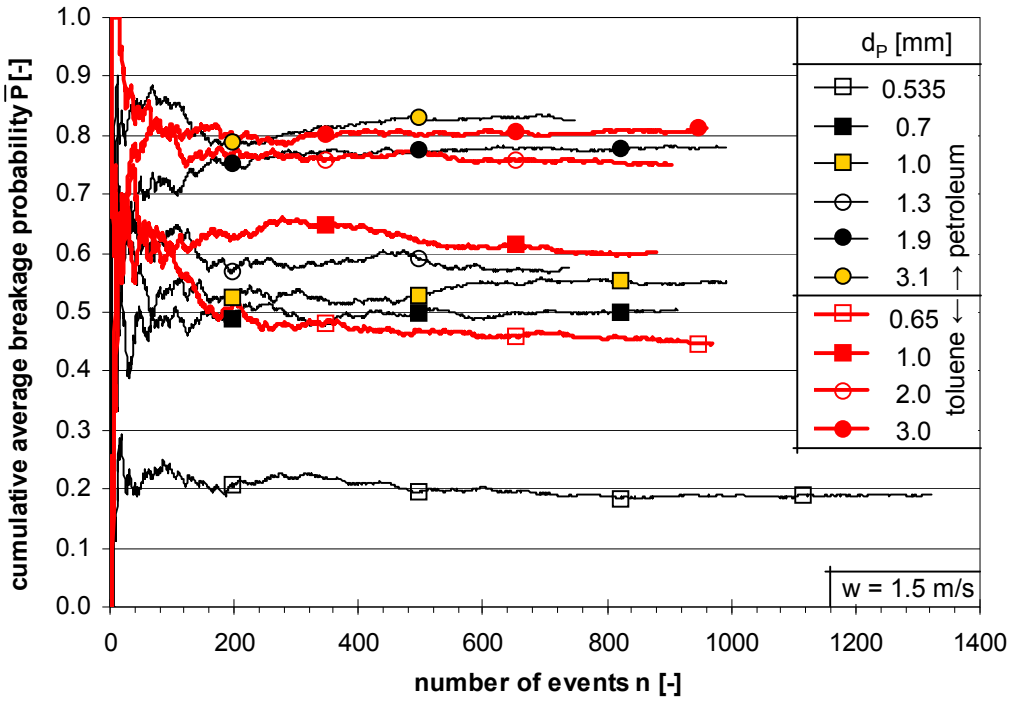

Figure 5 – Cumulative arithmetic average breakage probability as a function of analyzed breakage events of toluene and petroleum drops at a constant flow velocity for different mother drop diameter

The average values of the breakage probabilities are now compared with different model approaches from literature. The results for the petroleum drops are presented in Figure 6. All presented models follow the general trend of increasing probabilities with increasing mother drop diameter. After fitting the models against the experimental results, all three models propose a critical diameter for breakage in range of 100 - 200 µm. The experimental results around the 1.0 mm mother drop diameter are scattering, which makes it harder to find the optimal fitted set of parameters for the models. However, only the model of Alopaeus et al. (2002) scopes the increase of the probability for the least drops with satisfying results. The breakage probabilities proposed by Coulaloglou and Tavlarides (1977) and by Chen et al. (1998) over predicting the experimental results.

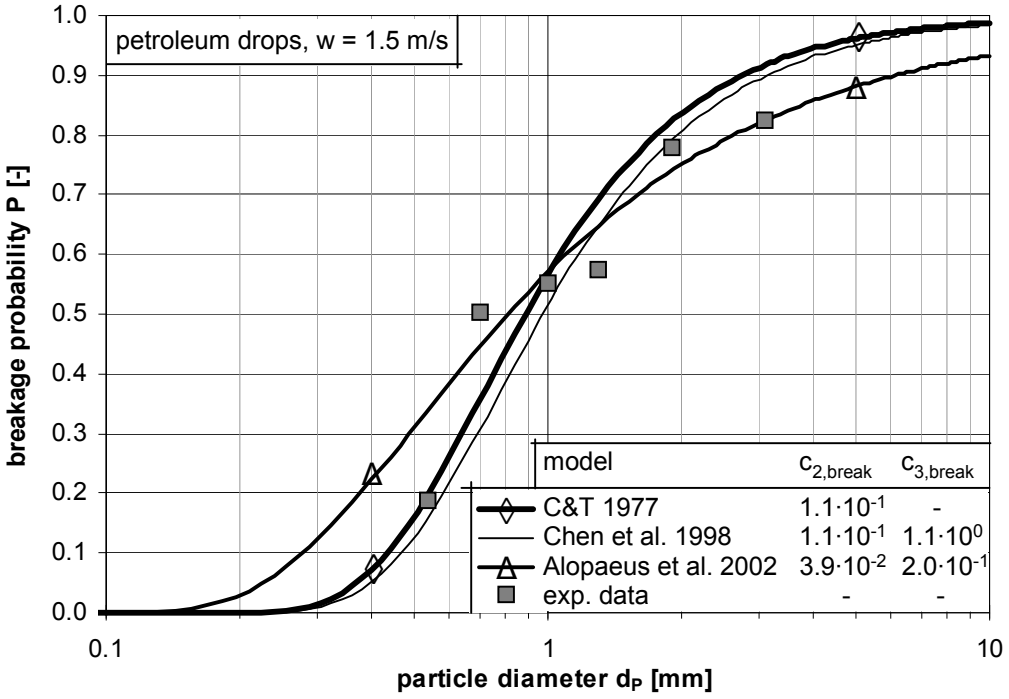

Figure 6 – Comparison of three breakage probability kernels with experimental single drop results for petroleum drops

The fitted parameters for each model approach are given in Figure 6. Note that the drawback of a second parameter in the model of Alopaeus et al. (2002) was avoided by keeping it constant to the value published in the original source. This leads to a negligible viscous force compared to the surface force of the petroleum drops. This is a reasonable assumption due to the low viscosities either of the petroleum as for the toluene drops. The fitted parameter $c_{2,break}$ is at the same order of magnitude as the published, optimized parameter by Alopaeus et al. (2002). An overview of all investigated parameters as a summary of used parameter values of the different models by several authors is given at the end of the study in Table 4. The value determined for $c_{2,break}$ = 0.08 in the model of Coulaloglou and Tavlarides (1977) is in good agreement with the range of parameter values given for this model in literature (see Table 4).

In Figure 7 the chosen parameters are also tested for and compared with the toluene probability results. The deviations between the experimental results and the model approaches by Coulaloglou and Tavlarides (1977) as the ones by Chen et al. (1998) are increasing with changing the dispersed phase system. Contrary the model of Alopaeus et al. (2002) perfectly predicts the experimental breakage probabilities. Due to the chosen parameters and thereby the subordinate role of the viscous forces, the structure of equation (8) is equal to the original model proposed by Narsimhan et al. (1979). A broad variation of the dispersed phase viscosity is necessary to determine the influence of surface tension versus viscosity in the right order of magnitudes.

Using the complete breakage rate of Alopaeus et al. (2002), Vankova et al. (2007) were not able to describe their data with a unique pair of values of the numerical

constants. The model did not merge towards a single curve of Vankova's various investigated systems. However, due to the success in literature and in this study we will consider the erfc-term from equation (8) as a robust model approach which describes breakage probabilities for a stirred vessel.

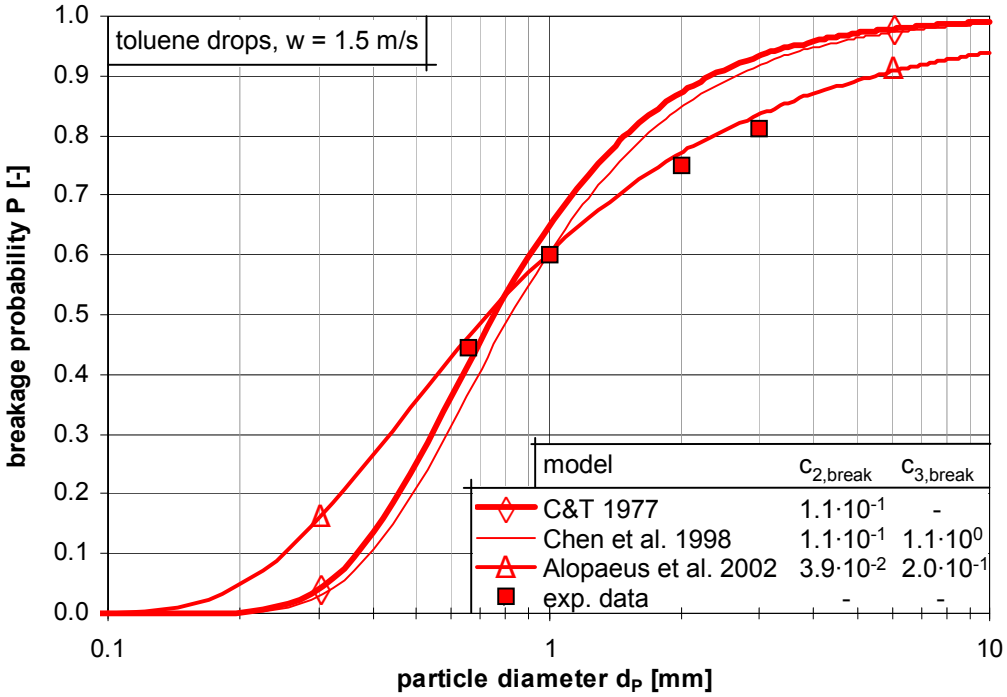

Figure 7 – Comparison of three breakage probability kernels with experimental single drop results for toluene drops

4.2 Breakage time

The discussion about the breakage time is much more controversy then the discussion about the breakage probability. Most of the contradicting opinions published were already presented in chapter 2.1 in this study. They will be evaluated with single drop experiments. Figure 8 presents the significance of the achieved experimental breakage times by cumulating the arithmetic average breakage time $\bar{t}_{break}$ over the number of events. Although the number of investigated events is much lower compared to Figure 5 (only the breaking drops are taken into account), all data sets run into a constant average value.

A general trend is hard to define, analyzing this average values. Three main theses can be point out: Firstly, the highest value of the breakage time for petroleum and toluene is always connected to the smallest mother drop diameter. Secondly, the average breakage time seems to have a minimum for a certain mother drop diameter. Thirdly, $\bar{t}_{break}$ of the toluene drops for a chosen diameter is always lower as for the petroleum drops with a comparable diameter. All those results have been achieved for a constant flow velocity of 1.5 m/s and therewith the average energy dissipation rate was constant for all experiments.

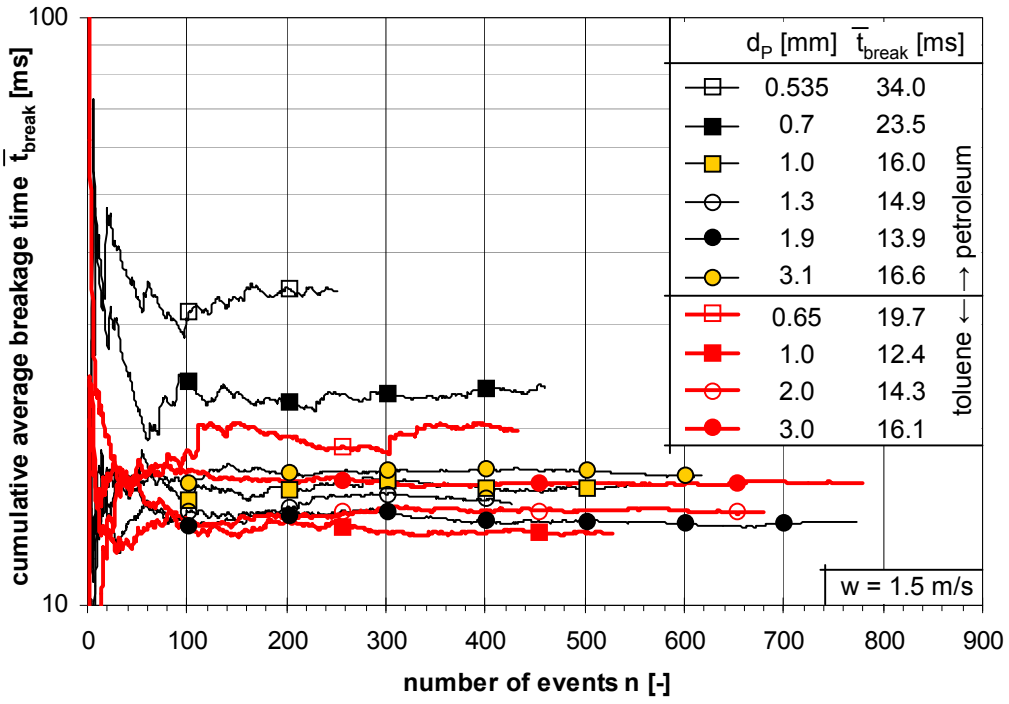

Figure 8 – Cumulative arithmetic average breakage time as a function of analyzed breakage events for a constant flow velocity and varying mother drop diameter

A more detailed differentiation is achieved by comparing the relative number distributions of the according average breakage times. The distribution corresponding to the highest (d_P = 0.535 mm) and the lowest (d_P = 1.9 mm) average breakage time are compared at a constant flow velocity in Figure 9. The distributions are not following a normal or a log-normal distribution around the arithmetic average value. Therefore they have been approximated with a β-distribution. The breakage time distribution resulting from the smaller diameter (d_P = 0.535 mm) is much wider than for the larger particle. As already mentioned in chapter 3.2 and displayed on Figure 3 – the small particles can have a really high residence time in the turbulent region behind the stirrer blade, until they break. The probability of a collision with an according eddy is decreasing with decreasing drop size. This stochastic phenomenon is already implemented in the breakage probability and displayed by lower values of the breakage probability for smaller particles then for large ones. However, the equal consideration of these extreme long breakage times, leads to a strong increase of the average value, especially for the smaller particles. The comparison of the maximum value of both distributions is much more revealing then the average value. Due to the unequal distributions of the number of events over the breakage time, the peak value of the corresponding β-distribution for the breakage time $\hat{t}_{break,\beta}$ of the 0.535 mm mother drops is 2.74 ms and for the 1.9 mm mother drops 9.88 ms. This interpretation of the breakage times seems much more reasonable to the authors then the use of the simple average value. The applicability of this method is shown in Figure 10.

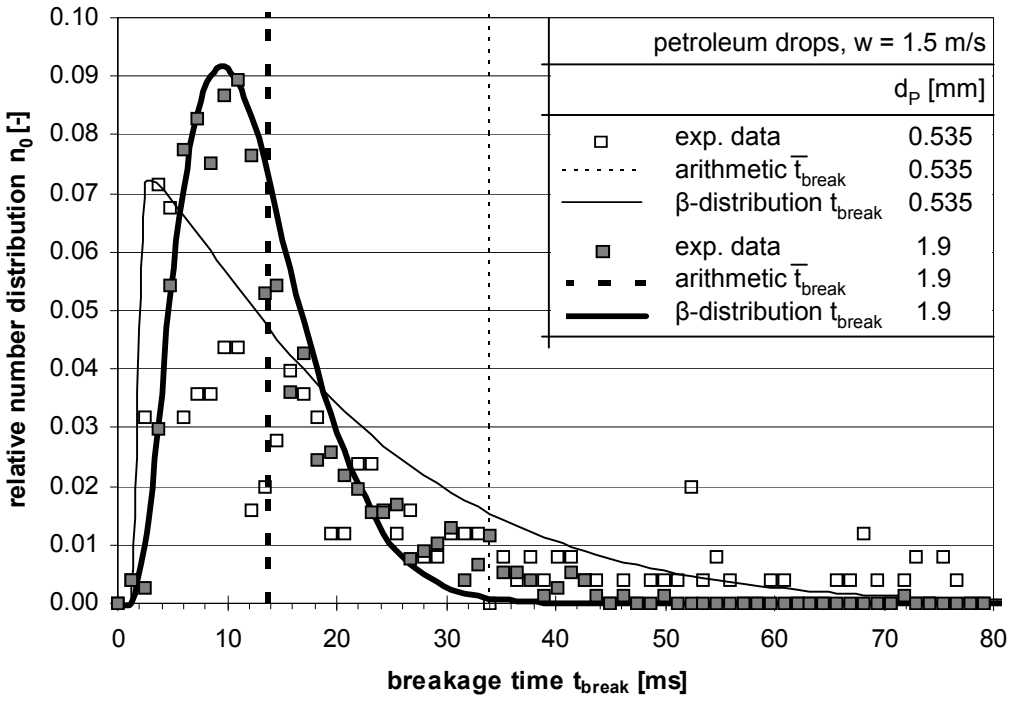

Figure 9 – Relative number distribution of the breakage time and its approximation with a β-distribution for two different petroleum mother drops at a constant flow velocity

For a constant flow velocity of 1.5 m/s, four breakage time distributions and their corresponding β-distributions are presented. The influence of the mother drop diameter and the dispersed phase is displayed. As shown in Figure 9, with increasing mother drop diameter the distributions become narrower and the peak values of the distributions are moving to larger breakage times. The toluene drops breaking always faster as the petroleum drops, due to their lower interfacial tension and viscosity.

The influence of the flow velocity on the breakage time is displayed in Figure 11. As expected with increasing flow velocity, the breakage time is decreasing. This is true for the average value as for the peak value of the corresponding β-distribution (compare also with Figure 14). The increase of the flow velocity increases the turbulence and therewith the velocities and the energies of the turbulent eddies. The drops are breaking more easy and faster. Note that the results for the toluene drops are again always smaller then the values for the breakage time of the petroleum drops.

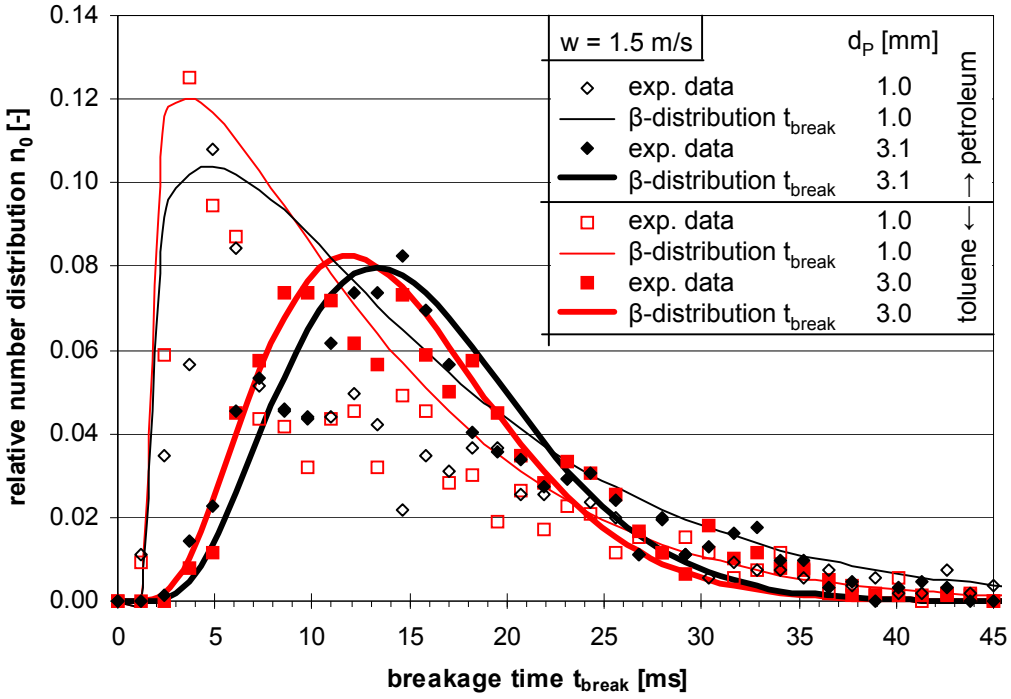

Figure 10 – Relative number distribution of the breakage time and its approximation with a β-distribution for different mother drops of petroleum and toluene

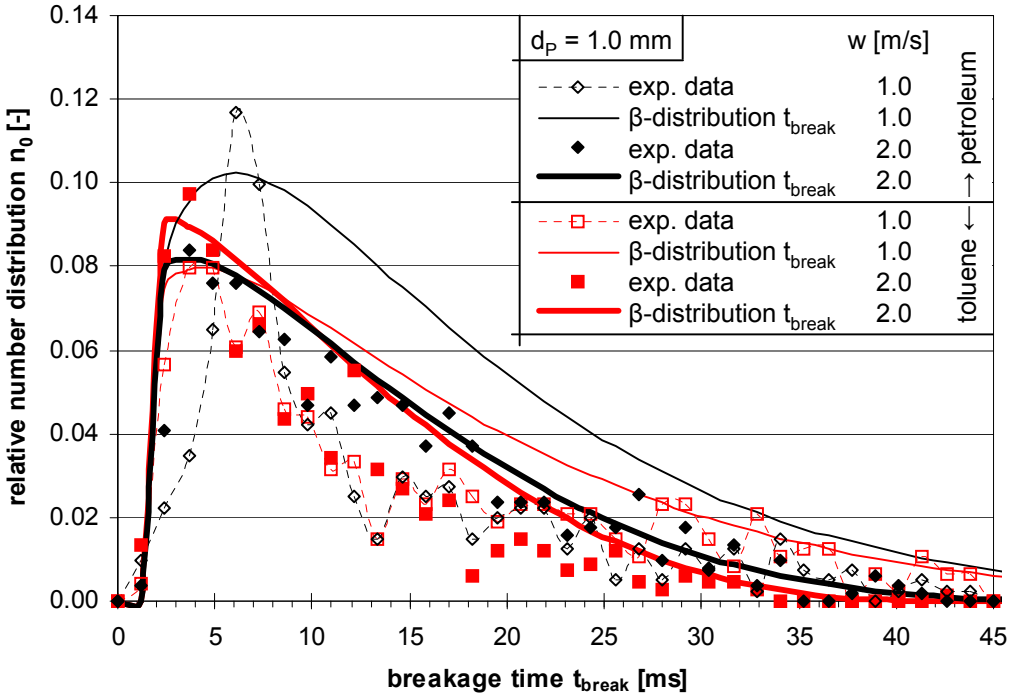

Figure 11 – Relative number distribution of the breakage time and its approximation with a β-distribution for a 1.0 mm mother drop diameter of petroleum and toluene at two different flow velocities

Several model from literature are compared with the experimental breakage times, based on this straight transformation results of $\bar{t}_{break}$ into a more meaningful $\hat{t}_{break,\beta}$. The development of modeled breakage times and a parameter magnitude analysis is shown in Figure 12 for the petroleum drops at a constant flow velocity of 1.5 m/s. Additionally the experimental results for the breakage time, both the average as the peak values of the β-distributions are compared with the theoretical values. All presented models propose a dependency of t_{break} on $(d_P)^{2/3}$ and display therewith the development of the $\hat{t}_{break,\beta}$ -values. With adaptation of the constants in the model, all three models are able to predict the development of the breakage time very well. The used constant for the correlation of the breakage rate is $1/c_{1,break}$, for comparison reason with known parameter values from literature, still $c_{1,break}$-values are shown in Figure 12. Although the absolute values for the measured breakage time, the average as the peak values, are in the same range like the ones reported in literature (Andersson and Andersson 2006; Konno et al. 1983), the magnitude of $c_{1,break}$-values are not. The optimized value of $c_{1,break}$ for the model of Coulaloglou and Tavlarides (1977) is one magnitude higher as the highest value reported in literature (see also Table 4). The lowest values reported in literature by Gäbler et al. (2006) are four magnitudes smaller then the values found here. Therewith their breakage time is four magnitudes higher then the observed one in this study. The authors are aware of the high challenges in parameter fitting for population balance equation and are not criticizing the earlier work of many work groups, but we propose always to compare the results of the parameter optimizations with the physical meaning of the optimized kernel. A value of $c_{1,break} = 10^{-4}$ leads to a breakage time for a 3.0 mm toluene drop of around 100 s at the investigated flow velocity of 1.5 m/s. This should be questioned and compared to the physical application of the simulation.

Further assumptions like the on from Chen et al. (1998) that t_{break} is a constant or from Alopaeus et al. (2002), who found no dependency of t_{break} on d_P can be considered as erroneous.

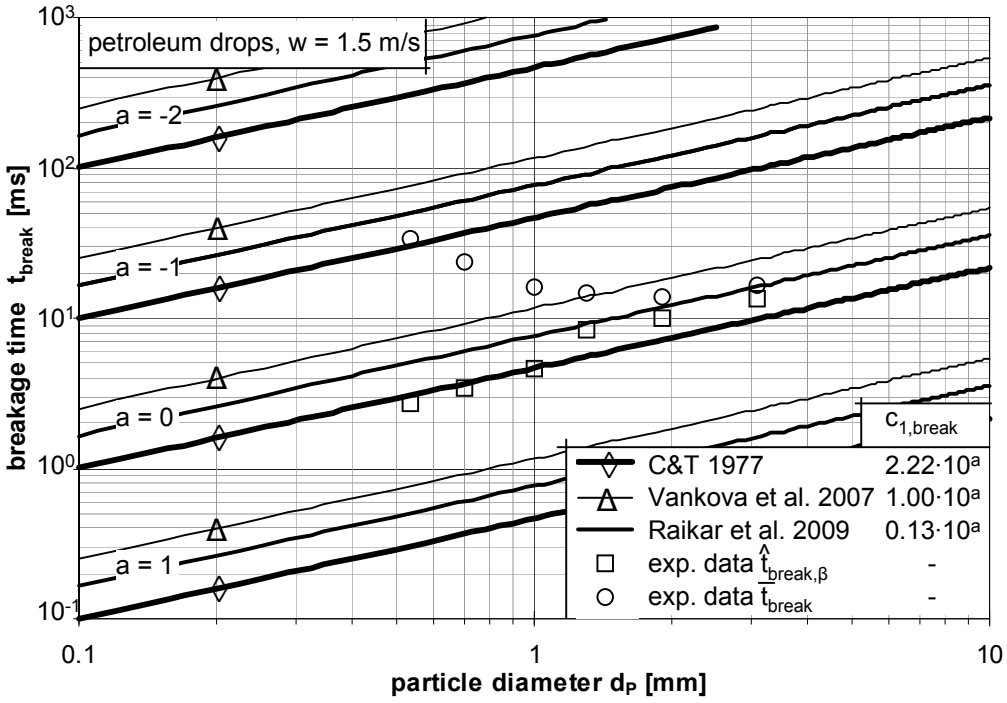

Figure 12 – Comparison of three breakage time kernels at different parameter magnitudes with experimental single petroleum drop results

The influence of the physical system on the breakage time is presented in Figure 13. The already discussed petroleum results are compared with the ones observed from the toluene drops. Additionally the two kinds of breakage time (average and peak values) are given for the toluene drops. Obviously the model of Coulaloglou and Tavlarides (1977) does not display the influence of physical properties on the breakage time. Therefore the model shows the same behavior for both systems. As discussed in chapter 2.1 the Vankova et al. (2007) and also Raikar et al. (2009) extended the traditional form from Coulaloglou and Tavlarides (1977) to take physical changes of the system into account. A comparison of equations (5) and (6) shows that both extensions contradict each other. While Raikar proposes an increasing breakage time with increasing dispersed density, Vankova et al. (2007) oppose that. They are considering proportionality between the deformation time of a drop and the density quotient of the liquid/liquid system. Furthermore they propose proportionality between the breakage time and the deformation time of a drop of a given size:

$$t_{break} \propto t_{deform} \propto \sqrt{\rho_c / \rho_d} \qquad (14)$$

The results for both extensions are given in Figure 13. The model proposed by Raikar et al. (2009) miss leads the prediction results by opposing the change direction. Therefore we will not consider this approach any further in this study. The extension of the breakage time model approach by Vankova et al. (2007), shown in equation (14), is an improvement. The optimized parameter $c_{1,break}$ is calculated out of the value for the model of Coulaloglou and Tavlarides (1977) and the viscosity ratio of water/petroleum to 2.5 (see also Table 4). Through that both breakage rates

give equal values for the petroleum system and Vankova et al. gives lower values for the toluene system, proven by the experimental results.

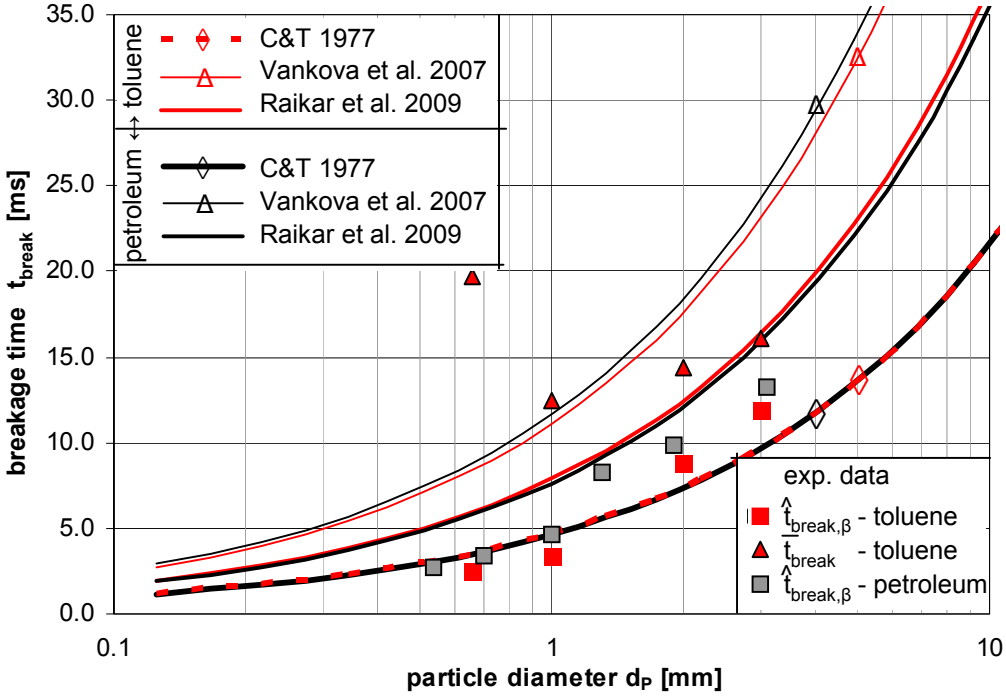

Figure 13 – Comparison of three breakage time kernels at different parameter magnitudes with experimental single toluene drop results, $c_{1,break}$ for all models as presented in Figure 12

The influence of the energy dissipation rate and therewith the flow velocity is presented in Figure 14. As expected, the breakage time is decreasing with increasing flow velocity. The dependency of t_{break} on $\varepsilon^{-1/3}$, derived from turbulence theory (Coulaloglou and Tavlarides 1977) could be shown for the average values as for the peak values of the breakage time. This dependency was already introduced in most of the model approaches. The presented model of Chen et al. (1998) neglects this dependency. Based on the results of the breakage probability and the breakage time, the breakage rate can be calculated out of the experimental data. A further comparison with theoretical model will lead to a clear judgment about the advantages and disadvantages of the different models as the experimental study.

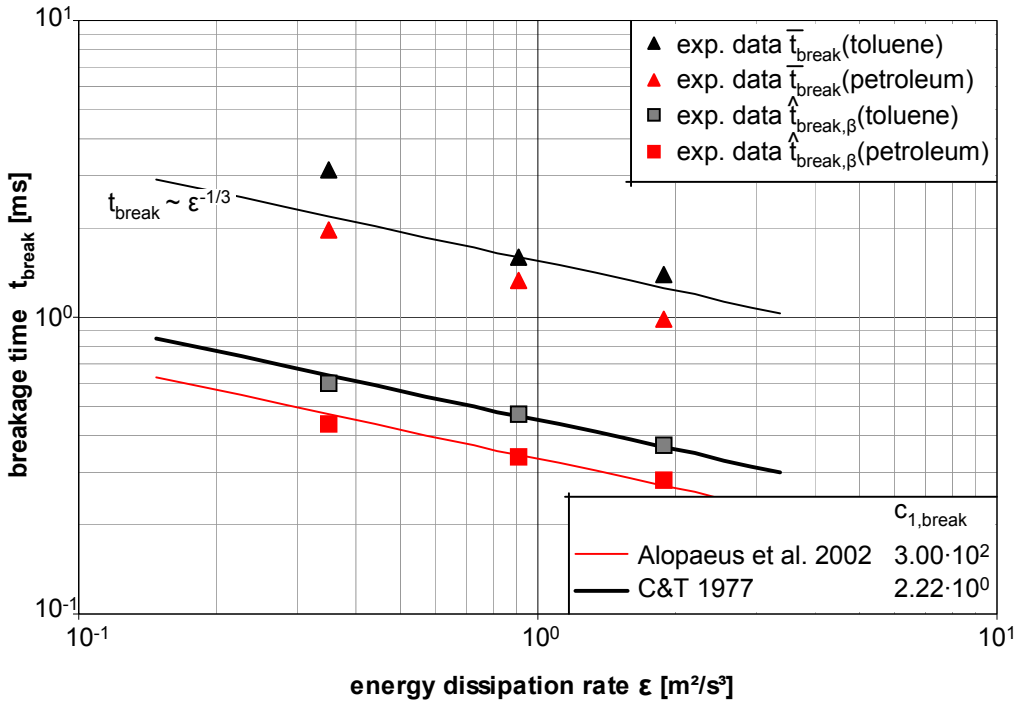

Figure 14 – Dependency of the breakage time on the energy dissipation rate, experimental and model results

4.3 Breakage rate

The breakage rate or breakage frequency is the most complex modeling approach in the breakage kernel within the PBM. The broad discussions about drop breakage mechanisms have lead into several contradicting models. No standard model could be defined already. In this study we want to achieve a clear statement about the qualitatively development of the breakage rate over the parent diameter and the energy dissipation rate. Furthermore we want to validate the different models on their prediction quality of changes in the physical properties. Due to the limited range of variation, using petroleum and toluene drops, this validation can only be a first hint and needs to be extended in further studies.

The comparison of experimental and theoretical breakage rates are given in Figure 15, at a constant flow velocity of 1.5 m/s, for the petroleum/water system. The used parameters in the models are presented in Table 4. The experimental data show clearly a maximum for the breakage rate around 0.7 mm due to the strong decrease of the inverse breakage time for increasing mother drop diameter. Monotone models like the ones by Chen et al. (1998) or Alopaeus et al. (2002) are not able to predict that behavior. While the model from Coulaloglou and Tavlarides (1977) displays qualitatively the experimental development, no unique pair of parameter values is able to predict the complete result range in a quantitative satisfying matter. The model of Martínez-Bazán et al. (1999) seems to give the best fit after fitting the parameter. Note that $c_{2,break}$, postulated as a theoretical constant equal 8.2, needed to be adapted for this study to 225. This is due to the differences in the turbulent field in this study compared to the original reference. The investigated pipe flow had much

higher values and a homogenous distribution of the energy dissipation rate. This is not the case in stirred vessels.

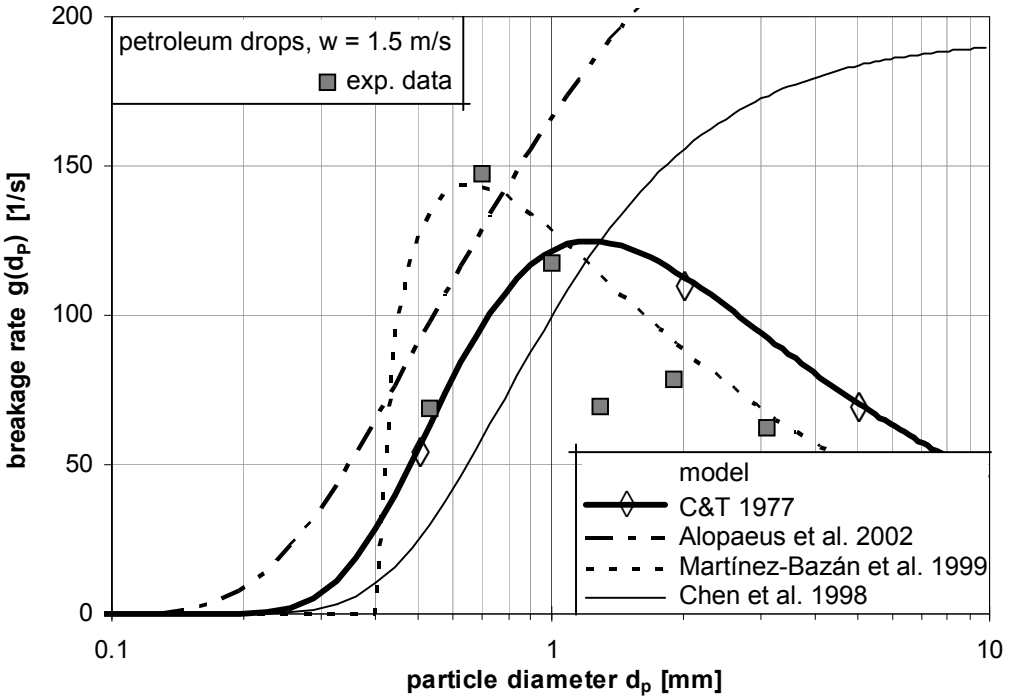

Figure 15 – Comparison of different breakage rates with experimental petroleum single drop experiments, the used parameters in the models are all given in Table 4 (this study)

For the further discussions, only the model approaches developing a maximum for a certain diameter will be taken into account. The comparison between the toluene and the petroleum system are shown in Figure 16. As a general trend, the models and the experiments show higher values for toluene then for petroleum at a given drop size. This increase by changing the physical system is only qualitatively well described by the model of Coulaloglou and Tavlarides (1977) as by Martínez-Bazán et al. (1999). Both models show to low maxima. A much better result is achieved by using the extended model from Vankova et al. (2007). The absolute values for the breakage rate maximum are met. The drawback is the width of the distribution. The experimental results show a narrow maximum peak and high gradients of both side of the maximum. This is only displayed by the model of Martínez-Bazán et al. (1999), which lacks a proper description of the influence of physical properties.

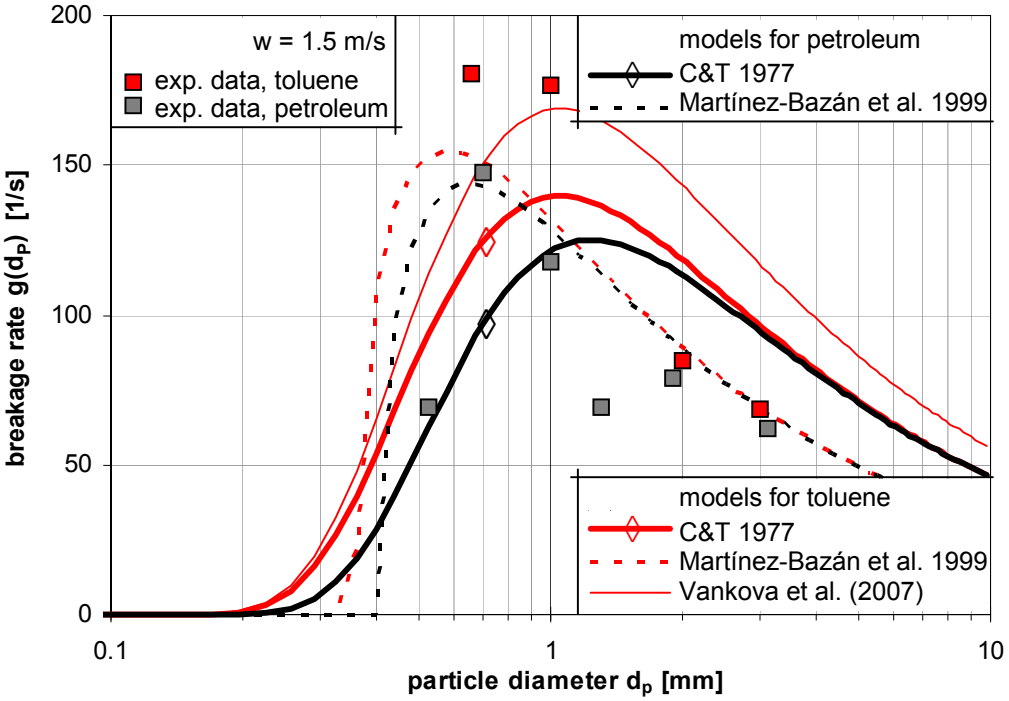

Figure 16 - Comparison of different breakage rates with experimental toluene and petroleum single drop experiments, the used parameters in the models are all given in Table 4 (this study)

Based on the results in chapter 4.1 and 4.2 the most significant changes should be made on the breakage time. There an influence of physical properties is not considered in most of the models. Vankova et al. (2007) propose two different proportionalities of physical parameters (η_d, ρ_d) on the drop deformation time, which can be directly related to the drop breakage time (see equation (14) & (15)) - the density ratio and the viscosity of the dispersed phase.

$$t_{break} \propto t_{deform} \propto \eta_d \qquad (15)$$

The importance of the PBM models is high but not absolute. Many different parameters are used in literature to adapt the model to experimental results. While transport, breakage and coalescence terms influence each other, different mathematical solutions are possible to display one set of experiments. To avoid a local optimum, simultaneous fitting, the use of different initial vales and a broad variation of the physical system are necessary but still not a guarantee. Transient measurements should be given a high weight in the fitting process in order to identify especially the breakage parameters properly (Maaß et al. 2010a). Still the fitting of PBM parameters is of major challenge and many physical influence parameters on drop sizes are still not implemented in the models or described properly. This all leads to a broad variety of parameters which is briefly summarized in Table 4. Many other studies have used the listed models but have not published their used

parameters. The whole PBM community would benefit, if that would become a standard for publishing PBM results.

The magnitudes of the parameter results achieved in this study show similar results to those in literature for the breakage probability ($c_{2,break}$ and $c_{3,break}$) and are always larger for the breakage time ($c_{1,break}$). While Martínez-Bazán et al. (1999) do not model the breakage rate based on probability theory for the distribution density of kinetic energy or velocity fluctuation, their parameters do not relate with breakage time or breakage probability. They have to be discussed separately from the others.

Table 4 – parameter listing

Literature reference	model displayed in equation	$c_{1,break}$	$c_{2,break}$	$c_{3,break}$
model from Coulaloglou and Tavlarides (1977)				
Coulaloglou and Tavlarides 1977	(4)	$3.36 \cdot 10^{-1}$	$1.06 \cdot 10^{-1}$	-
Ross et al. 1978	(4)	$4.87 \cdot 10^{-3}$	$8.00 \cdot 10^{-2}$	-
Hsia and Tavlarides 1983	(4)	$1.03 \cdot 10^{-2}$	$6.35 \cdot 10^{-2}$	-
Bapat and Tavlarides 1985	(4)	$4.81 \cdot 10^{-3}$	$8.00 \cdot 10^{-2}$	-
Gäbler et al. 2006	(4)	$6.14 \cdot 10^{-4}$	$5.70 \cdot 10^{-2}$	-
Maaß et al. 2010a	(4)	$1.40 \cdot 10^{-2}$	$3.33 \cdot 10^{-1}$	-
this study	(4)	$2.22 \cdot 10^{0}$	$1.10 \cdot 10^{-1}$	-
model form Vankova et al. (2007)				
Vankova et al. 2007	(5)	$3.30 \cdot 10^{-2}$	$3.60 \cdot 10^{0}$	-
this study	(5)	$2.50 \cdot 10^{0}$	$1.10 \cdot 10^{-1}$	-
model from Chen et al. (1998)				
Chen et al. 1998	(7)	$6.04 \cdot 10^{-1}$	$1.14 \cdot 10^{-3}$	$7.85 \cdot 10^{-3}$
Ruiz and Padilla 2004	(7)	$4.40 \cdot 10^{-1}$	$5.00 \cdot 10^{-3}$	$5.00 \cdot 10^{-3}$
this study	(7)	not determined	$1.10 \cdot 10^{-1}$	$1.10 \cdot 10^{0}$
model from Alopaeus et al. (2002)				
Alopaeus et al. 2002	(8)	$3.68 \cdot 10^{0}$	$7.75 \cdot 10^{-2}$	$2.00 \cdot 10^{-1}$
Gäbler et al. 2006	(8)	$3.63 \cdot 10^{-3}$	$2.49 \cdot 10^{-4}$	$7.24 \cdot 10^{-2}$
Singh et al. 2009	(8)	$7.70 \cdot 10^{0}$	$1.50 \cdot 10^{-2}$	$1.00 \cdot 10^{-2}$
this study	(8)	$3.00 \cdot 10^{2}$	$3.90 \cdot 10^{-2}$	$2.00 \cdot 10^{-1}$
model from Martinez-Bazan et al. 1999				
Martínez-Bazán et al. 1999	(9)	$2.50 \cdot 10^{-1}$	$8.20 \cdot 10^{0}$	-
this study	(9)	$1.00 \cdot 10^{-1}$	$2.25 \cdot 10^{2}$	-

4.4 Number of daughter drops

In the PBM formulations the number of daughter fragments determines the average number of daughter particles v produced by breakage of a parent particle size d_P. The breakage of a parent drop d_P into two daughter drops d'_P and d''_P is assumed in most investigations reported (Raikar et al. 2009). The choice of the number of daughter particles directly influences the other breakage model parts in the PBM framework (Ramkrishna 2000). It is obvious, that the change of v or the daughter drops size distribution $\beta(d_p,d'_p)$ will directly effect the breakage rate $g(d_P)$ and therewith always the numerical parameters.

The experimentally determined number of daughter particles during the first breakage process is presented as a function of the system and the mother drop diameter for a constant flow velocity in Figure 17. As a general trend, the initial number of daughter drops is decreasing with increasing mother drop diameter. For the smallest investigated drop diameter, petroleum drops with d_P = 0.535 mm, the probability for an initial binary breakage is over 95%. This probability is decreasing to almost 70% for the 3.1 mm petroleum as for the 3.0 mm toluene drop. The table in Figure 17 also displays the average number of particles out of all breakage events for a constant flow velocity and a diameter of a given size. Additionally the maximum numbers of daughter drops counted for one initial single breakage event are given in the table in Figure 17.

The highest numbers are always connected to the largest mother drops. Note that for the toluene drops of a comparable size to the petroleum drops, the number of daughter fragments is always slightly higher.

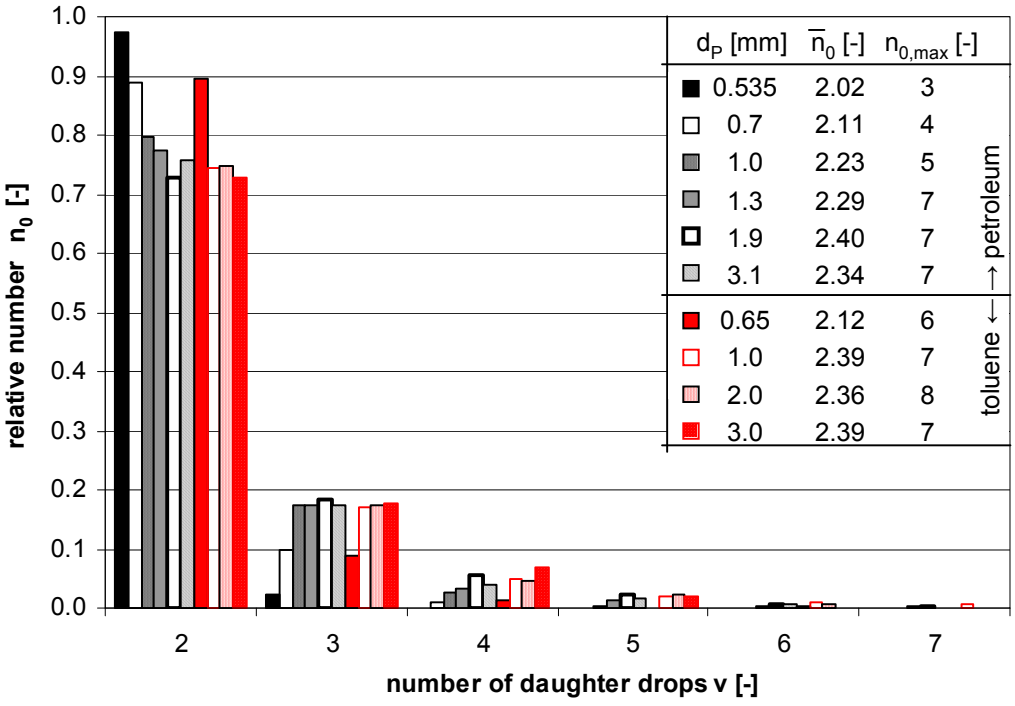

Figure 17 – relative number distribution over the initial number of daughter drops after the first breakage event at a constant flow velocity of 1.5 m/s

The explanations for the achieved results are exemplarily discussed in Figure 18. The figure shows a breakage sequence of a breaking 2 mm toluene mother drop for 1.5 m/s. The flow direction is displayed in frame 14 of the set. Although the drop is extremely elongated and stretched, the first breakage occurring is a binary (see frame 14 in Figure 18). Note that the second number behind the image number on each frame displays the number of particles counted in those images. The breakage process is going on and the maximum number of particles is increasing. Also ternary or even higher breakage events occur (see frame 15 in Figure 18). This breakage cascade leads to the maximum number of drops at one image in frame 23 with 27 particles. A frame rate not with 822 fps but with 822/23 fps would have seen a breakage event with 27 particles. This sequence shows the influence of the measurement technique on the achieved results. Additionally all ternary or higher breakage events are most probably binary breakages. To observe this, a much higher time resolution is necessary then the used one.

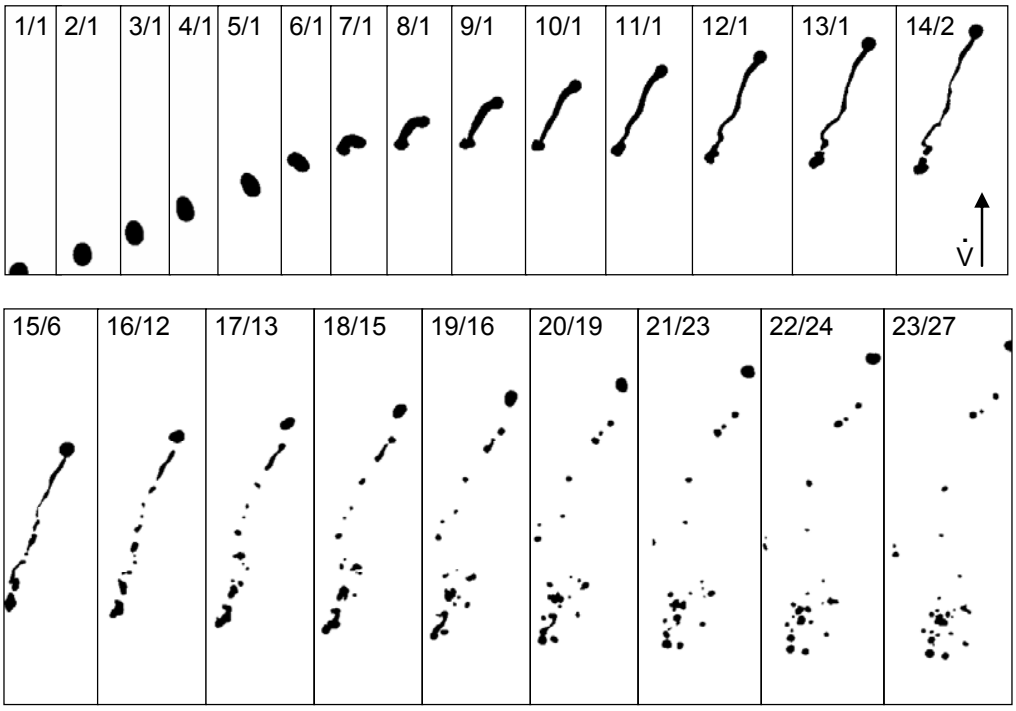

Figure 18 – Example initial binary breakage with following break-up cascade of 2 mm toluene drop, always with the image number/ number of particles on the image

The results for the maximum number of daughter drops for both systems at a constant flow velocity are shown in Figure 19. The distribution of the number of particles is much wider then the one presented in Figure 17. As expected much higher numbers are achieved for all diameters. The maximum number of particles found in on experiments set is given as the average number from this set. Again both numbers are always higher for the toluene system and increase with increasing drop diameter.

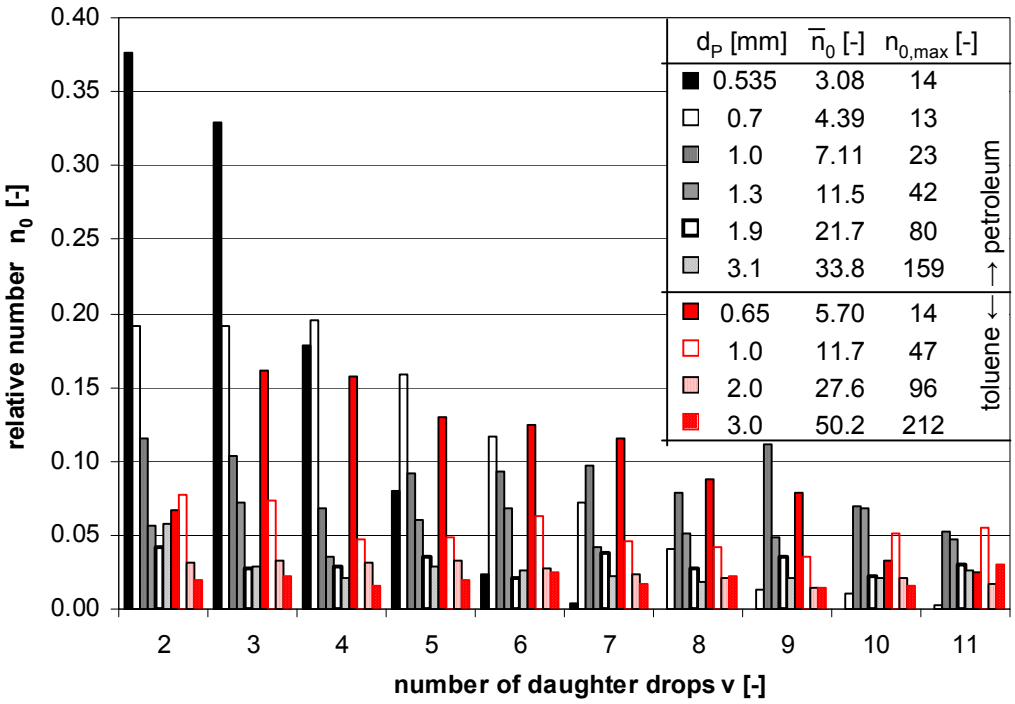

Figure 19 – relative number distribution over the maximum number of daughter drops measured at one point in time at a constant flow velocity of 1.5 m/s

5 Conclusion

In this study, detailed and precise parameter determination for the PBM models of the breakage rates have been analyzed separately from coalescence in a single drop breakage cell. Therefore the breakage time and the breakage probability of toluene and petroleum drops have been studied using high-speed imaging. Additionally the number of daughter fragments occurring in single drop breakage events has been observed. All results have been compared with values from literature. The single drop experiments support the assumption of binary breakage as of increasing breakage time with increasing mother drop diameter.

Acknowledgements

The authors gratefully acknowledge the efficient support by the DAAD students Ms. Sarah Turner and Ms. Jennifer Komaiko, also the DAAD for the financial support via the RISE program and Ms. Gottschling for the great cooperation over the last years. We additionally thank Ms. Melanie Zillmer for the full automation of the image analysis.

This work was supported by the “Max-Buchner-Forschungsstiftung”.

Symbols

c concentration [g/L]

c	proportionality or numerical constant
d_{32}	Sauter mean diameter [m]
d_P	particle, mother drop diameter [m]
d'_P, d''_P	daughter drop diameter
H	liquid level of the stirred vessel [m]
n_0	relative number distribution [-]
P	breakage probability [-]
T	vessel diameter [m]
t	time [s]
t_b	breakage time [s]
$\bar{t}_{break}$	arithmetic average breakage time [s]
$\hat{t}_{break,\beta}$	peak value of the β-distribution of the breakage time [s]
w	flow velocity [m/s]
β	daughter drop size distribution [-]
γ	interfacial tension [N/m]
ε	energy dissipation rate [m²/s³]
η	dynamic viscosity [Pa·s]
φ	dispersed phase fraction [-]
ν	number of daughter drops [-]
ρ	density [kg/m³]

Abbreviations

C&T 1977	Coulaloglou and Tavlarides (1977)
fps	frames per second
PBM	population balance modeling

Literature

Alopaeus, V., Koskinen, J., Keskinen, K.I. and Majander, J., 2002. Simulation of the population balances for liquid-liquid systems in a nonideal stirred tank. Part 2 - parameter fitting and the use of the multiblock model for dense dispersions. Chemical Engineering Science, 57(10): 1815-1825.

Andersson, R. and Andersson, B., 2006. On the breakup of fluid particles in turbulent flows. Aiche Journal, 52(6): 2020-2030.

Bahmanyar, H. and Slater, M.J., 1991. Studies of drop break-up in liquid-liquid systems in a rotating disc contactor. Part I: Conditions of no mass transfer. Chemical Engineering and Technology, 14(2): 79-89.

Bapat, P.M. and Tavlarides, L.L., 1985. Mass-Transfer in a Liquid-Liquid Cfstr. AIChE Journal, 31(4): 659-666.

Batchelor, G.K., 1952. Diffusion in a field of homogeneous turbulence: II. The relative motion of particles. Mathematical Proceedings of the Cambridge Philosophical Society, 48: 345-362.

Batchelor, G.K., 1956. The Theory of Homogenous Turbulence. Cambridge University Press.

Calabrese, R.V., Chang, T.P.K. and Dang, P.T., 1986. Drop Breakup in Turbulent Stirred-Tank Contactors .1. Effect of Dispersed-Phase Viscosity. Aiche Journal, 32(4): 657-666.

Chatzi, E. and Lee, J.M., 1987. Analysis of Interactions for Liquid Liquid Dispersions in Agitated Vessels. Industrial & Engineering Chemistry Research, 26(11): 2263-2267.

Chen, Z., Pruss, J. and Warnecke, H.J., 1998. A population balance model for disperse systems: Drop size distribution in emulsion. Chemical Engineering Science, 53(5): 1059-1066.

Coulaloglou, C.A. and Tavlarides, L.L., 1977. Description of Interaction Processes in Agitated Liquid-Liquid Dispersions. Chemical Engineering Science, 32(11): 1289-1297.

Eastwood, C.D., Armi, L. and Lasheras, J.C., 2004. The breakup of immiscible fluids in turbulent flows. Journal of Fluid Mechanics, 502: 309-333.

Gäbler, A., Wegener, M., Paschedag, A.R. and Kraume, M., 2006. The effect of pH on experimental and simulation results of transient drop size distributions in stirred liquid-liquid dispersions. Chemical Engineering Science, 61(9): 3018-3024.

Galinat, S., Masbernat, O., Guiraud, P., Dalmazzone, C. and Nolk, C., 2005. Drop break-up in turbulent pipe flow downstream of a restriction. Chemical Engineering Science, 60(23): 6511-6528.

Hancil, V. and Rod, V., 1988. Break-up of a Drop in a Stirred Tank. Chemical Engineering and Processing, 23(3): 189-193.

Hill, P.J. and Ng, K.M., 1995. New Discretization Procedure for the Breakage Equation. AIChE Journal, 41(5): 1204-1216.

Hsia, M.A. and Tavlarides, L.L., 1983. Simulation analysis of drop breakage, coalescence and micromixing in liquid-liquid stirred tanks. The Chemical Engineering Journal, 26(3): 189-199.

Jon, D.I., Rosano, H.L. and Cummins, H.Z., 1986. Toluene Water/1-Propanol Interfacial-Tension Measurements by Means of Pendant Drop, Spinning Drop, and Laser Light-Scattering Methods. Journal of Colloid and Interface Science, 114(2): 330-341.

Konno, M., Aoki, M. and Saito, S., 1983. Scale Effect on Breakup Process in Liquid Liquid Agitated Tanks. Journal of Chemical Engineering of Japan, 16(4): 312-319.

Kuriyama, M., Ono, M., Tokanai, H. and Konno, H., 1995. The Number of Daughter Drops Formed Per Breakup of a Highly Viscous Mother-Drop in Turbulent-Flow. Journal of Chemical Engineering of Japan, 28(4): 477-479.

Lasheras, J.C., Eastwood, C., Martinez-Bazan, C. and Montanes, J.L., 2002. A review of statistical models for the break-up of an immiscible fluid immersed into a fully developed turbulent flow. International Journal of Multiphase Flow, 28(2): 247-278.

Liao, Y. and Lucas, D., 2009. A literature review of theoretical models for drop and bubble breakup in turbulent dispersions. Chemical Engineering Science, 64(15): 3389-3406.

Liao, Y. and Lucas, D., 2010. A literature review on mechanisms and models for the coalescence process of fluid particles. Chemical Engineering Science, 65(10): 2851-2864.

Maaß, S., Gäbler, A., Zaccone, A., Paschedag, A.R. and Kraume, M., 2007. Experimental investigations and modelling of breakage phenomena in stirred liquid/liquid systems. Chemical Engineering Research & Design, 85(A5): 703-709.

Maaß, S., Wollny, S., Sperling, R. and Kraume, M., 2009. Numerical and experimental analysis of particle strain and breakage in turbulent dispersions. Chemical Engineering Research and Design, 87(4): 565–572.

Maaß, S., Metz, F., Rehm, T. and Kraume, M., 2010a. Prediction of drop sizes for liquid/liquid systems in stirred slim reactors part I: Single stage impellers. Chemical Engineering Journal, 162: 792-801.

Maaß, S., Wollny, S., Voigt, A. and Kraume, M., 2010b. Experimental comparison of measurement technique for drop size distributions in liquid/liquid dispersions. Experiments in Fluids, article in press, DOI: 10.1007/s00348-010-0918-9: 11 pp.

Maaß, S., Rojahn, J. and Kraume, M., 2011. Automated image analysis for in-situ observation and control of multiphase dispersions occurring in chemical and process engineering. submitted to: Advanced Powder Technology, 22(2)

Martínez-Bazán, C., Montanés, J.L. and Lasheras, J.C., 1999. On the breakup of an air bubble injected into a fully developed turbulent flow. Part 1. Breakup frequency. Journal of Fluid Mechanics, 401: 157-182.

Narsimhan, G., Gupta, J.P. and Ramkrishna, D., 1979. Model for Transitional Breakage Probability of Droplets in Agitated Lean Liquid-Liquid Dispersions. Chemical Engineering Science, 34(2): 257-265.

Raikar, N.B., Bhatia, S.R., Malone, M.F. and Henson, M.A., 2009. Experimental studies and population balance equation models for breakage prediction of emulsion drop size distributions. Chemical Engineering Science, 64(10): 2433-2447.

Ramkrishna, D., 2000. Population balances, theory and applications to particulate systems in engineering. Academic Press, San Diego, CA, 355 pp.

Rodríguez-Rodríguez, J., Gordillo, J.M. and Martínez-Bazán, C., 2006. Breakup time and morphology of drops and bubbles in a high-Reynolds-number flow. Journal of Fluid Mechanics, 548: 69-86.

Ross, S.L., Verhoff, F.H. and Curl, R.L., 1978. Droplet Breakage and Coalescence Processes in an Agitated Dispersion. 2. Measurement and Interpretation of Mixing Experiments. Industrial & Engineering Chemistry Fundamentals, 17(2): 101-108.

Ruiz, M.C. and Padilla, R., 2004. Analysis of breakage functions for liquid-liquid dispersions. Hydrometallurgy, 72(3-4): 245-258.

Sathyagal, A.N., Ramkrishna, D. and Narsimhan, G., 1995. Solution of Inverse Problems in Population Balances .2. Particle Break-Up. Computers & Chemical Engineering, 19(4): 437-451.

Shinnar, R., 1961. On the Behaviour of Liquid Dispersions in Mixing Vessels. Journal of Fluid Mechanics, 10(2): 259-275.

Singh, K.K., Mahajani, S.M., Shenoy, K.T. and Ghosh, S.K., 2009. Population Balance Modeling of Liquid-Liquid Dispersions in Homogeneous Continuous-Flow Stirred Tank. Industrial & Engineering Chemistry Research, 48(17): 8121-8133.

Thoroddsen, S.T., Etoh, T.G. and Takehara, K., 2008. High-speed imaging of drops and bubbles. Annual Review of Fluid Mechanics, 40: 257-285.

Tsouris, C. and Tavlarides, L.L., 1994. Breakage and Coalescence Models for Drops in Turbulent Dispersions. AIChE Journal, 40(3): 395-406.

Vankova, N., Tcholakova, S., Denkov, N.D., Vulchev, V.D. and Danner, T., 2007. Emulsification in turbulent flow 2. Breakage rate constants. Journal of Colloid and Interface Science, 313(2): 612-629.

Villermaux, E., 2007. Fragmentation. Annual Review of Fluid Mechanics, 39: 419-446.

Windhab, E.J., Dressler, M., Feigl, K., Fischer, P. and Megias-Alguacil, D., 2005. Emulsion processing - from single-drop deformation to design of complex processes and products. Chemical Engineering Science, 60(8-9): 2101-2113.